

# FEM Simulation of Non-Axisymmetric Stretch Flange Forming of Aluminum Alloy 5052 Based on Shell Type Elements

Y. Dewang<sup>1,\*</sup>, M. S. Hora<sup>2</sup> and S. K. Panthi<sup>3</sup>

\* [yogesh\\_dewang@yahoo.co.in](mailto:yogesh_dewang@yahoo.co.in)

Received: July 2017

Accepted: November 2017

<sup>1</sup> Department of Mechanical Engineering, Lakshmi Narain College of Technology, Bhopal, India.

<sup>2</sup> Department of Civil Engineering, Maulana Azad National Institute of Technology, Bhopal, India.

<sup>3</sup> CSIR- Advanced Materials and Processes Research Institute (CSIR-AMPRI), Bhopal, India.

DOI: 10.22068/ijmse.14.4.69

**Abstract:** Finite element simulation of stretch flanging process was carried out in order to investigate the effect of process parameters on maximum thinning (%) in stretch flanging process. Influences of initial flange length, punch die clearance, width of sheet metal blank and blank holding force were investigated on maximum thinning (%). Finite element simulation was done using FEM software package ABAQUS. Sheet metal blanks of AA 5052 were utilized for numerical simulation of stretch flanging process. Mesh convergence study was carried out to ascertain the accuracy of present FEM model. It is found that circumferential strain and shell thickness decreases with decrease in initial flange length and punch-die clearance while both decreases with increase in blank-holding force. Radial strain increases with decrease in initial flange length and punch-die clearance and with increment in blank-holding force and width of sheet. It is found that width of sheet metal blank and blank holding force have greater influence on maximum thinning (%) as compared to initial flange length and punch die clearance.

**Keywords:** Flanging, Thinning, Initial flange length, Punch die clearance.

## 1. INTRODUCTION

Metal forming is one the prime mode for forming the metals into useful form through application of forces. Basically, metal forming comprises of bulk metal forming and sheet metal forming technologies. Bulk metal forming includes processes such as extrusion, rolling, drawing and forging etc. while on the other hand sheet metal forming includes processes like deep drawing, flanging, hemming, electromagnetic forming etc. Application of FEM simulation is an efficient tool for analysis of metal forming processes for obtaining defect free products with improved quality. Researchers had worked for analysis of metal forming processes by using FEM simulation in past. Radial forward extrusion is analyzed by using FEM simulation software namely ABAQUS [1]. FEM procedures were also utilized for calculation of dislocation density in different regions of a deformed workpiece of 99.99% pure copper during forming process [2]. In the area of sheet metal forming processes, it is found that through FEM simulation that forming depth increased considerably in

electromagnetic forming process by using a sheet on a convex punch instead of using a sheet into a concave die [3].

Flanging is one of the important sheet metal forming processes. It is widely applied in automobile and stamping industries for making hidden joints and assembly of automobile parts. Products obtained by flanging have smooth rounded edge, higher rigidity or strength to the edge of sheet-metal parts. Stretch flanging is one of the major type of flanging process. Many researchers in past have studied various aspects of stretch flanging which include theoretical, experimental and numerical studies. A 3D finite element analysis of stretch curved flanging was carried out and considered the effect of length of straight side, radius of curved range, flange height, and curvature radius of punch [4]. Numerical and analytical study was carried out on stretch flanging of V-shaped shaped metal using elastic-plastic FEM program in which the effect of normal anisotropy, strain hardening exponent, flange angle, flange length are considered [5]. A forward-inverse prediction scheme was presented that combines explicit

**Table 1.** Values of properties of AA 5052 used as input for FEM simulation

S.No.	Property	Magnitude
1.	Mass density	2680 kg/m <sup>3</sup>
2.	Young's Modulus	70.3 GPa
3.	Poisson's ratio	0.33

dynamic finite element method (FEM), true strain method (TSM), and adaptive-network-based fuzzy inference system (ANFIS) in order to determine the anisotropic optimum blank in stretch flange process [6]. A multi-scale finite element damage percolation model was employed to simulate stretch flange forming of AA 5182 and AA 575 [7]. Numerical simulation of stretch flange forming of Al–Mg sheet AA5182 was performed using the upper and lower bound constitutive models of Garson–Overgaard–Needleman (GTN) and Sun and Wang, respectively [8]. A continuum mechanics based approach was utilized for prediction of radial and circumferential crack in AA 5182 stretch flanges on the basis of extended stress-based forming limit curve [9]. Influence of initial flange length and punch-die clearance on circumferential strain distribution and radial strain distribution are studied in stretch flanging process of AA 5052 using finite element simulation [10].

In view of literature mentioned above, it can be concluded that majority of researchers utilized FEM technique for analysis of various forms of stretch flanging using other aluminum alloy, but none of them focused to capture the deformation behavior of AA 5052 sheets in terms of percentage of thinning for non-axisymmetric stretch flanging process specifically through two dimensional shell (S4R) elements. The aim of present study is to simulate non-axisymmetric stretch flanging of AA 5052 alloy of 0.5 mm thickness using commercial software package ABAQUS by using 2D shell elements.

In present investigation, FEM simulation of non-axisymmetric stretch flanging process is carried out to study the effect of process parameters such as initial flange length, punch die clearance, blank holding force and width of

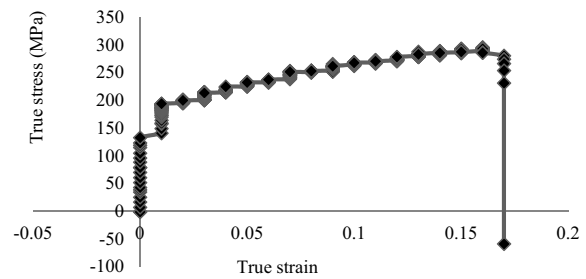


**Fig. 1.** True stress-strain curve for AA 5052

sheet metal blank on maximum thinning occurred in stretch flange forming using shell elements.

## 2. MATERIALS BEHAVIOR

The mechanical properties of aluminum alloy 5052 sheet by preparing tensile test samples as per standard methods of tension testing method E8/E8M–11 ASTM [11]. The tensile specimens were tested on a computerized universal testing machine at a strain rate of 0.16667 per second. The true stress- strain curve obtained from tensile test is shown in Fig. 1. Table 1 shows values of properties of AA 5052 used as input for FEM simulation.

### 2. 1. FINITE ELEMENT MODELLING

#### 2. 1. 1. FEM Model

Finite element simulations of stretch flanging process are performed using commercially available software ABAQUS. The values of properties of AA 5052 used as input for FEM simulation are given in Table 1. The isotropic hardening rule is considered for the material which behaves as elastic-plastic material. The

meshed FEM model meshed of die consists of the following dimensions: radius of die = 35 mm, 30 mm, 25 mm & 20 mm, height of die = 80 mm, fillet radius at all radii = 5 mm. Meshing of die is done with a 3D shell type feature which consists of R3D4 discrete rigid element type. It has 2734 elements and 2785 nodes. It is meshed by free meshing technique. Another meshed model is of punch which has dimensions: radius of punch=30 mm, height of die = 55 mm, fillet radius = 5 mm. It is a shell type feature which consists of 4429 R3D4 quadrilateral discrete rigid elements and 4485 nodes. Blank holder has dimensions in terms of radius as 20mm, 25mm, 30 mm and 35 mm. It is also discretized using 448 R3D4 discrete rigid elements and 492 nodes. Dimensions of sheet metal blank are as: length of sheet metal blank = 100 mm, width of sheet metal blank = 50 mm, thickness of sheet metal blank = 0.5 mm. The blank of AA 5052 is considered as deformable entity. The blank is modeled using a 4-node doubly curved thin shell element with reduced integration, S4R finite strain elements having 5 integration points through thickness. It consists of 7770 S4R quadrilateral discrete rigid

elements and 7952 nodes. The blank-holder is then allowed to move in the vertical direction to accommodate changes in the blank thickness. The friction coefficient of 0.1 was defined between different contact surfaces. The die remains fixed in all direction while sheet was allowed as a free body which was controlled by the contact boundary condition between the different tools and sheet. The punch movement was defined using a pilot node. This node is employed to obtain the punch force to bend the sheet during simulation. Punch was allowed to move only in downward direction while it was constrained in all other direction. Finite element simulations are done using radius of die and holder=30 mm in the present study.

### 2. 1. 2. Mesh Sensitivity & Convergence Analysis

In order to evaluate the sensitivity of mesh, five different mesh sizes are considered namely 40\*40, 50\*40, 60\*40, 70\*40 and 80\*40 as shown in Fig. 2. The mesh convergence is evaluated in terms of output parameters such as radial strain, circumferential strain, von-Mises stress,

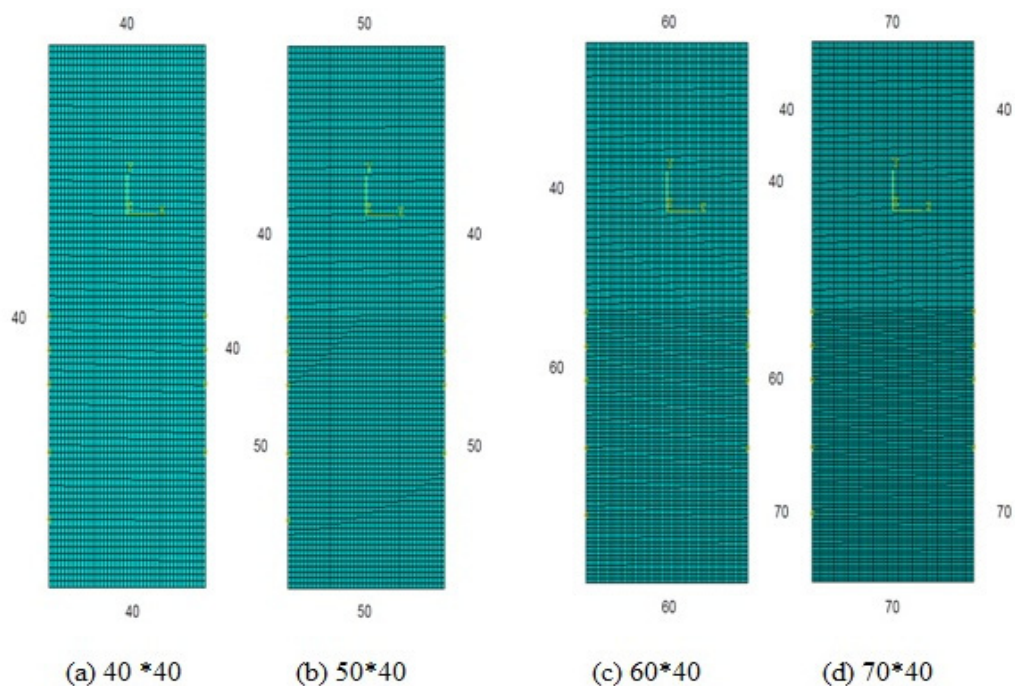


**Fig. 2.** Different mesh sizes for the mesh sensitivity and convergence (a)40\*40 (b)50\*40 (c)60\*40 (d)70\*40 (e)80\*40

**Table 2.** Mesh convergence data

S.No.	Mesh size	CPU time (sec)	Total no. of elements	Max. von-Mises stress (N/mm <sup>2</sup> )	Max. radial strain	Maximum hoop strain (max.)	Shell thickness (mm) (min.)
1	40*40	9705	10812	284.5	0.0498	0.0854	0.517
2	50*40	15402	12112	286.9	0.0500	0.0959	0.463
3	60*40	22420	13612	284.8	0.0506	0.099	0.462
4	70*40	32420	15312	286.1	0.0517	0.099	0.464
5	80*40	44136	17212	286.3	0.0425	0.100	0.464

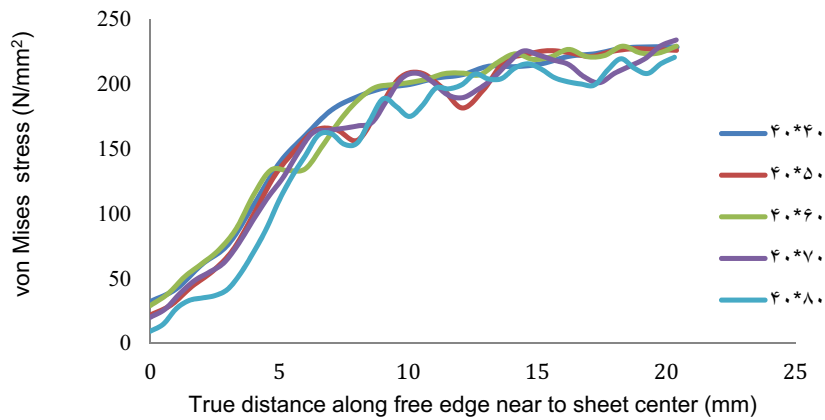


**Fig. 3.** von-Mises stress distribution for different mesh sizes

flange thickness. Table 2 shows the mesh convergence study data with total computational time. It clearly indicates that convergence is obtained for the partitioned mesh size 60\*40 with lesser computational time. Figure 3 shows that the von mises stress converged for the mesh size of 60\*40 and 70\*40. That is why, 60\*40 mesh size is selected out of 70\*40 mesh size, as it involves less number of elements and less computational time at the expense of reasonable accuracy. In this way as the all the output parameters converges for the mesh size 60\*40. Therefore for this mesh size 60\*40, mesh convergence is reported.

**2. 1. 3. Finite Element Modeling with Shell Elements**

This section describes the development of finite element model for non-axisymmetric stretch flanging process using shell type elements. In the current work, one of the shell

elements used is known as S4R. It is used for discretization of blank of Aluminum alloy in FEM analysis. S4R is a 4-noded quadrilateral element with reduced integration rule with one integration point. It is robust and generally used for a wide range of applications. This element is present in commercial software package ABAQUS and based on thick shell theory. It considers finite-strain formulation and thus can

be used to perform large strain analyses. It has the feature of uniformly reduced integration to avoid shear and membrane locking. It converges to shear flexible theory for thick shells and classical theory for thin shells. Fig. 4 shows the four node shell element (S4R).

It is a 3D shell type feature which consists of R3D4 discrete rigid element type. It has 2734 elements and 2785 nodes and is meshed by free meshing technique. It is a shell type feature which consists of 448 R3D4 discrete rigid elements and 492 nodes. It is meshed by free meshing technique. Punch is meshed with shell

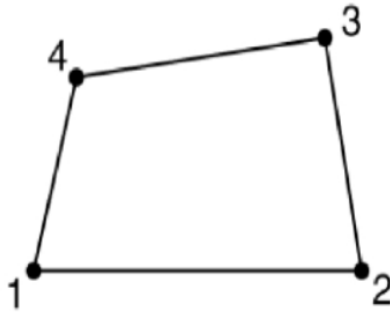


Fig. 4. A 4-node (S4R) shell element type

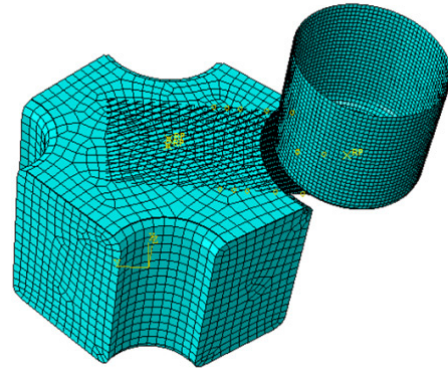


Fig. 5. Finite element model for stretch flanging process

type feature which consists of 4429 R3D4 quadrilateral discrete rigid elements and 4485 nodes. The blank is considered as deformable entity. The blank is modeled using a 4-node, doubly curved, thin shell element with reduced integration, S4R finite strain elements having 5 integration points through thickness. It consists of 7770 S4R quadrilateral discrete rigid elements and 7952 nodes. Fig. 5 shows the finite element model of stretch flanging process with blank discretized with S4R elements.

### 3. RESULTS & DISCUSSION

#### 3. 1. Effect of Blank Holding Force

Fig. 6 shows the effect of constant blank holding force on radial strain distribution along

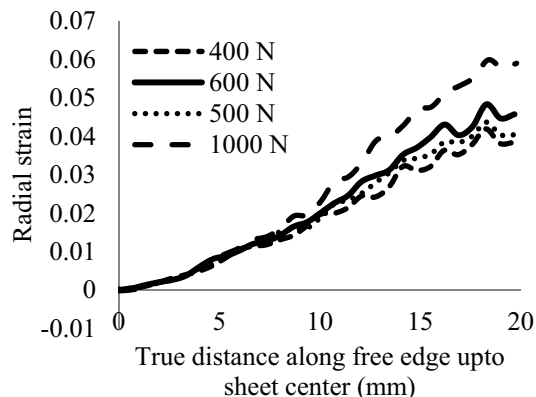


Fig. 6. Effect of blank holding force on radial strain

free edge.

It is found that radial strain increases with increase in constant blank holding force. It is important to notice that the maximum radial strain and the minimum radial strain are found at the center of the free edge and corner edge of stretch flange respectively for all cases. The increment in the radial strain upon increment in blank holding with constant intensities is basically due to the increment in greater capacity to hold the blank and which would increase the coefficient of friction between blank and other interacting surfaces.

Fig. 7 shows the effect of constant blank holding forces on circumferential strain. It is found that circumferential strain increases with increase in blank holding force and attains its maximum value for the maximum blank holding

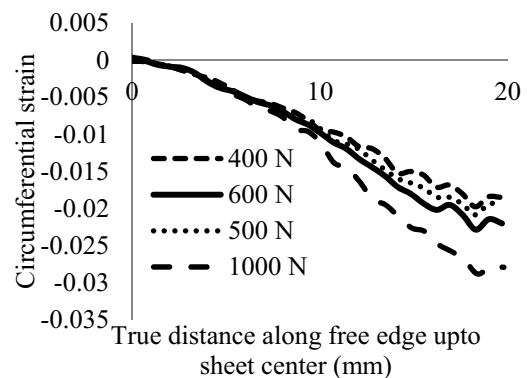


Fig. 7. Effect of blank holding force on circumferential strain

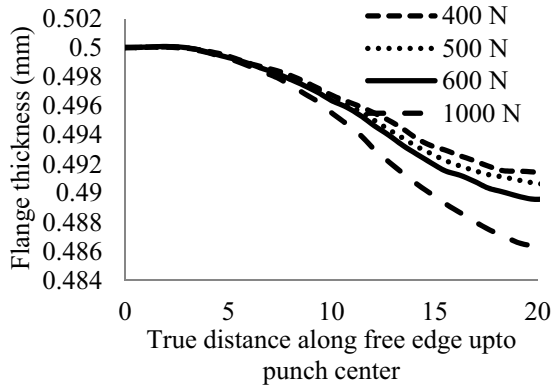


Fig. 8. Effect of blank holding force on flange thickness

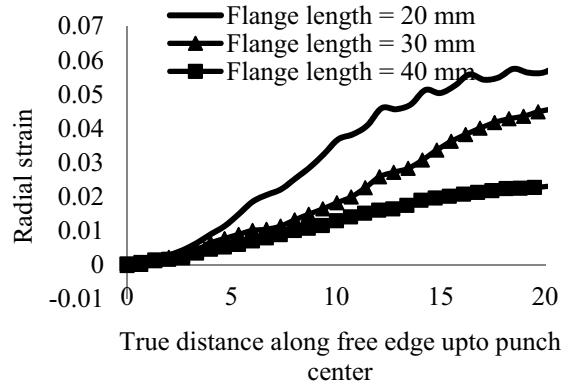


Fig. 9. Effect of initial flange length on radial strain

force. The circumferential strain is found to be maximum at free edge of blank and minimum at the centre of sheet metal blank for all cases. The contributing factor here for the increment of circumferential strain along free edge of blank is the coefficient of friction which act between blank, die, blank holder and punch. Upon increment of blank holding forces the circumferential strain increases in which friction coefficient helps in holding and forming the stretch flange with greater induced circumferential strain.

Fig. 8 shows the variation of flange thickness along free edge of stretch flange upto punch center for different blank holding forces of constant intensity. It is found that the flange

thickness varies non-linearly from free edge of flange to sheet center. The minimum flange thickness is obtained at the center of sheet. The greater will be the blank holding force the higher will be the reduction in flange thickness at center of sheet. The reduction in flange thickness is occurring due to the effect of the blank holding force as greater will be the blank holding force, the effect of coefficient of friction also contributes for reduction in flange thickness.

### 3. 2. Effect of Initial Flange Length

This section presents finite element simulation results pertaining to the effect of initial flange length on output parameters such as radial strain,

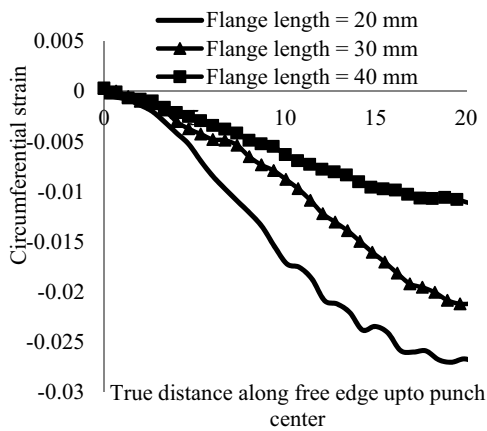


Fig. 10. Effect of initial flange length on circumferential strain

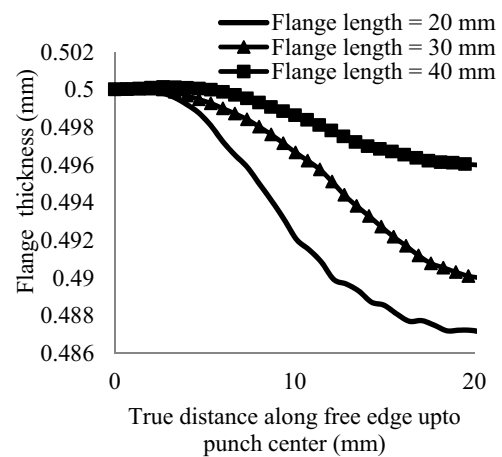


Fig. 11. Effect of initial flange length on flange thickness

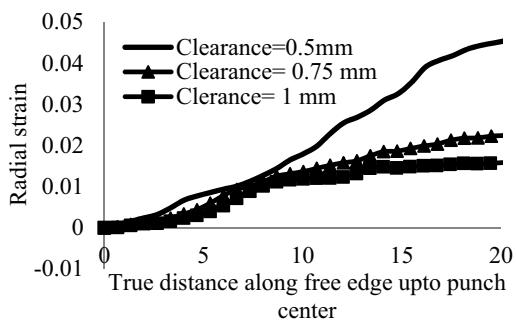
circumferential strain and flange thickness. It is found from Fig. 9 and Fig. 10 that circumferential strain increases while radial strain decreases with increase in initial flange length. It is also noticeable that the maximum radial strain and the maximum circumferential strain are obtained at the sheet center and corner edge of flange respectively. The increment in circumferential strain and decrement in radial strain along free edge of sheet upto sheet center is due to increment in initial flange length. The increase in initial flange length corresponds to the availability of greater amount of length for deformation and hence greater contact area is available due to which the circumferential strain increases and radial strain decreases along free edge of sheet to sheet center. The greater degree of deformation and increment in circumferential strain and decrement in radial strain is also due to coefficient of friction. Therefore the circumferential strain increases and radial strain decreases along free edge and maximum circumferential strain and maximum radial strain is found at corner of flange.

Fig. 11 shows the effect of initial flange length on flange thickness. It is found that that the flange thickness varies non-linearly along the free edge. The flange thickness is found maximum at the corner of the free edge while minimum at the center of the free edge for all initial flange length values. It is found that with increase in initial flange length results in diminishing flange thickness variation. Upon increment of initial flange length the reduction in flange thickness

reduces along free edge to sheet center. This might be occurring due to the increment in initial flange length as result of which for a given blank holding force, the reduction in flange thickness will be less as more amount of blank holding force will be required to hold it and then to further deform it, to obtain change in thickness of flange and lower will be the initial flange length, higher will be reduction in flange thickness along free edge to sheet center. Therefore higher will be the initial flange length, the reduction in thickness will be lesser.

### 3. 3. Effect of Punch-Die Clearance

This section presents finite element simulation results that represent the effect of punch -die clearance on output parameters, such as radial strain, circumferential strain, flange thickness. Fig. 12 and Fig. 13 shows the effect of punch-die clearance on radial strain and circumferential strain. It is found that radial strain decreases while circumferential strain increases with increment of punch-die clearance. The maximum radial strain and the maximum circumferential strain are obtained at the center of sheet and free edge of sheet. It is noticeable that little decrement in circumferential strain is observed at free edge with increase in punch-die clearance while a considerable decrement is observed in circumferential strain with increase in punch-die clearance at centre of sheet. The circumferential strain and radial strain both decreases with increase in punch die clearance because with



**Fig. 12.** Effect of punch-die clearance on radial strain

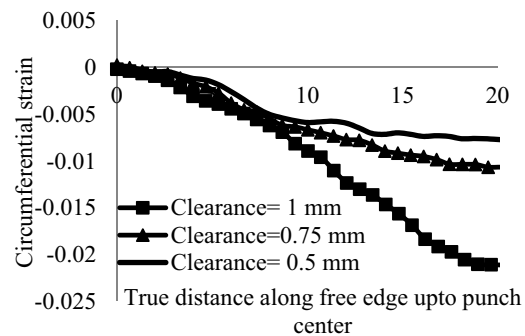


**Fig. 13.** Effect of punch-die clearance on circumferential strain

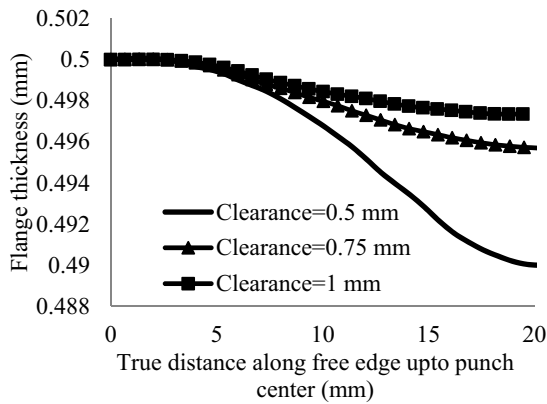


Fig.14. Effect of punch-die clearance on flange thickness

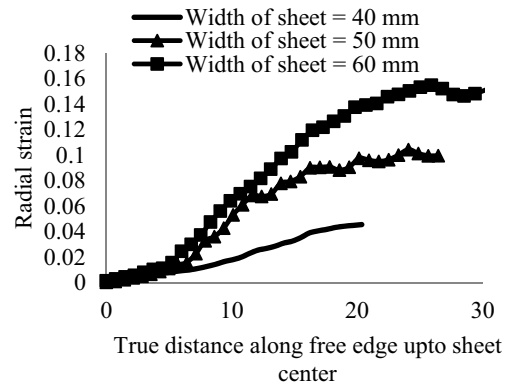


Fig.15. Effect of width of sheet metal blank on radial strain

increase in punch die clearance the gap between the punch and sheet for deformation increases which actually decreases the effective force which is required to form the stretch flange. The lesser will be the punch-die clearance the higher will be the radial strain and circumferential strain at sheet center and corner edge of flange respectively. Again here, coefficient of friction also plays role in stretch flange forming. Fig. 14 shows the effect of punch-die clearance on flange thickness. It is found that flange thickness varies non-linearly along the free edge of blank. The flange thickness is found maximum at the corner of flange while it is minimum at the center of the sheet. The reduction in flange thickness along free edge to sheet center decreases with increase in punch die clearance. This might be occurring due to the fact that higher will be the punch die clearance the reduction(change) in flange thickness will be lower because the combined effect of given blank-holding force and coefficient of friction reduces to form the stretch flange with higher strain values. Therefore the reduction in flange thickness decreases with increase in punch-die clearance.

### 3. 4. Effect of Width of Sheet Metal Blank

The variation of radial strain, circumferential strain, and flange thickness, with distance along free edge up to sheet center is investigated for different values of sheet width. Fig. 15 and Fig. 16 show the effect of width of blank on radial

strain and circumferential strain distribution along free edge of sheet. It is found that radial strain and circumferential strain increases non-linearly with increase in the width of sheet. It is important to notice that the maximum radial strain and the maximum circumferential strain are obtained for largest width of sheet. The maximum radial strain is found at center of sheet while maximum circumferential strain occurs at the corner edge of sheet. The increment in radial strain as well as in circumferential strain along free edge of sheet with increase in width of sheet is occurring due to increment in width of sheet because the sheet with greater width provides the chances of greater degree of deformation. The

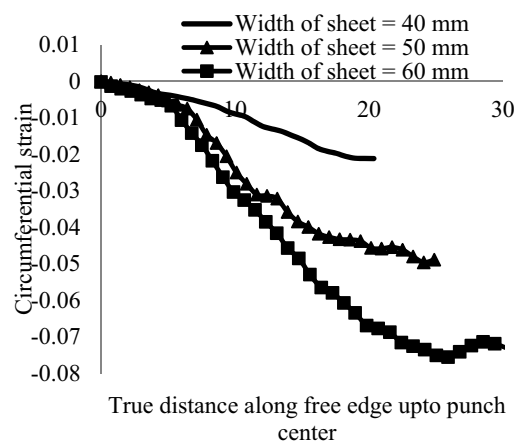


Fig. 16. Effect of width of sheet metal blank on circumferential strain

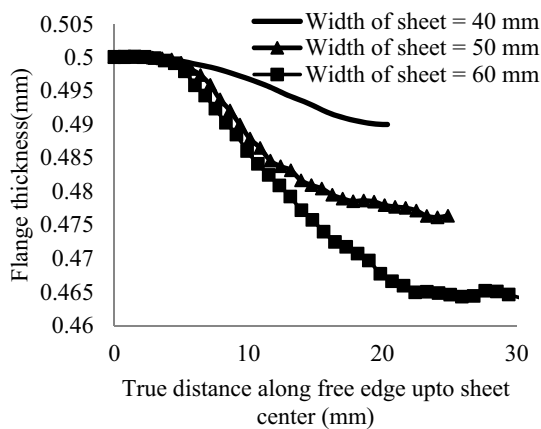


Fig. 17. Effect of width of sheet metal blank on flange thickness

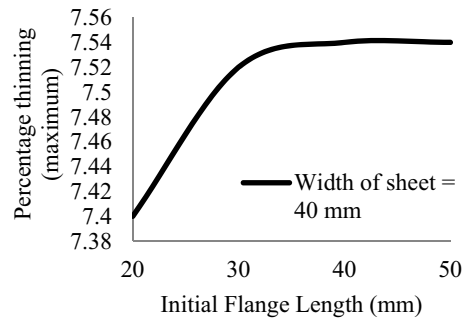


Fig. 18. Effect of initial flange length on percentage of thinning(maximum)

lesser will be width of sheet, it is rather difficult to deform it into flange as well as the strain induced after flange formation will also be less. The combined effect of blank holding force and coefficient of friction also plays important role as well. Therefore the radial strain and circumferential strain both increases with increment in width of sheet.

Fig. 17 shows the effect of width of blank on flange thickness variation. It is found that the flange thickness increases with increase in the width of blank at corner edge of flange. The minimum flange thickness value is obtained for the least sheet width. The flange thickness of 50 mm and 60 mm sheet width values are pretty close to each other and far apart from their corresponding values for the sheet width of 40 mm. Besides this, it is also found that the reduction in flange thickness along free edge up to punch center is found to increase with increase in width of sheet. The minimum thickness for the greatest width is found at the sheet center because due to increment in width of blank greater degree of deformation appeared at the sheet center and again due to combined effect of given blank holding force and coefficient of friction minimum flange thickness is obtained.

### 3. 5. Effect of Process Parameters on Percentage of Thinning (Maximum)

This section describes the effect of different process parameters such as initial length, punch-

die clearance, blank-holding force and width of blank on percentage of thinning (maximum). The percentage of thinning (maximum) can be computed with usage of simplified formula as:

$$\text{Percentage of thinning (maximum)} = \frac{((\text{Final thickness of blank} - \text{Initial thickness of blank}))}{(\text{Initial thickness of blank})}$$

Percentage of thinning (maximum) for different process parameters is shown in Table 3.

Fig.18 to Fig. 21 shows the effect of process parameters such as initial flange length, punch-die clearance, blank-holding force and width of blank on percentage of thinning (maximum) respectively.

It is found from the figures that percentage of thinning increases with increase in initial flange

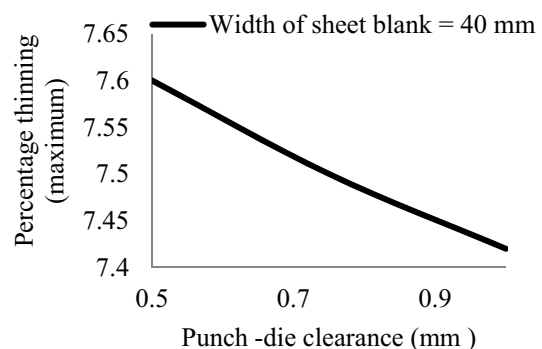


Fig. 19. Effect of punch-die clearance on percentage of thinning(maximum)

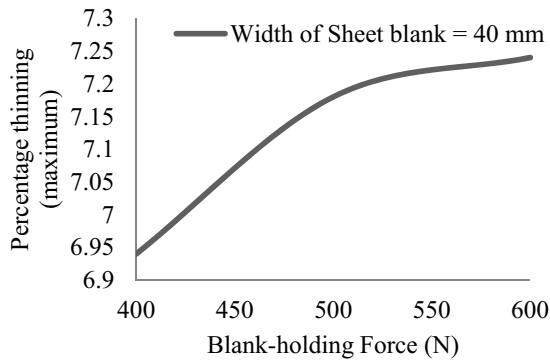


Fig. 20. Effect of blank - holding force on percentage of thinning

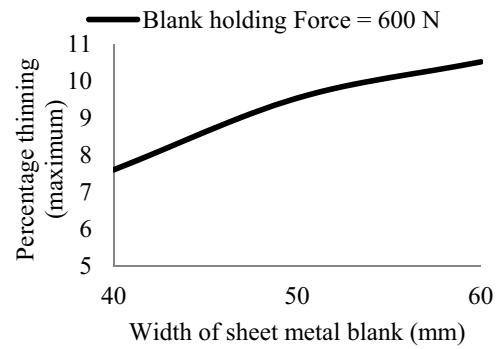


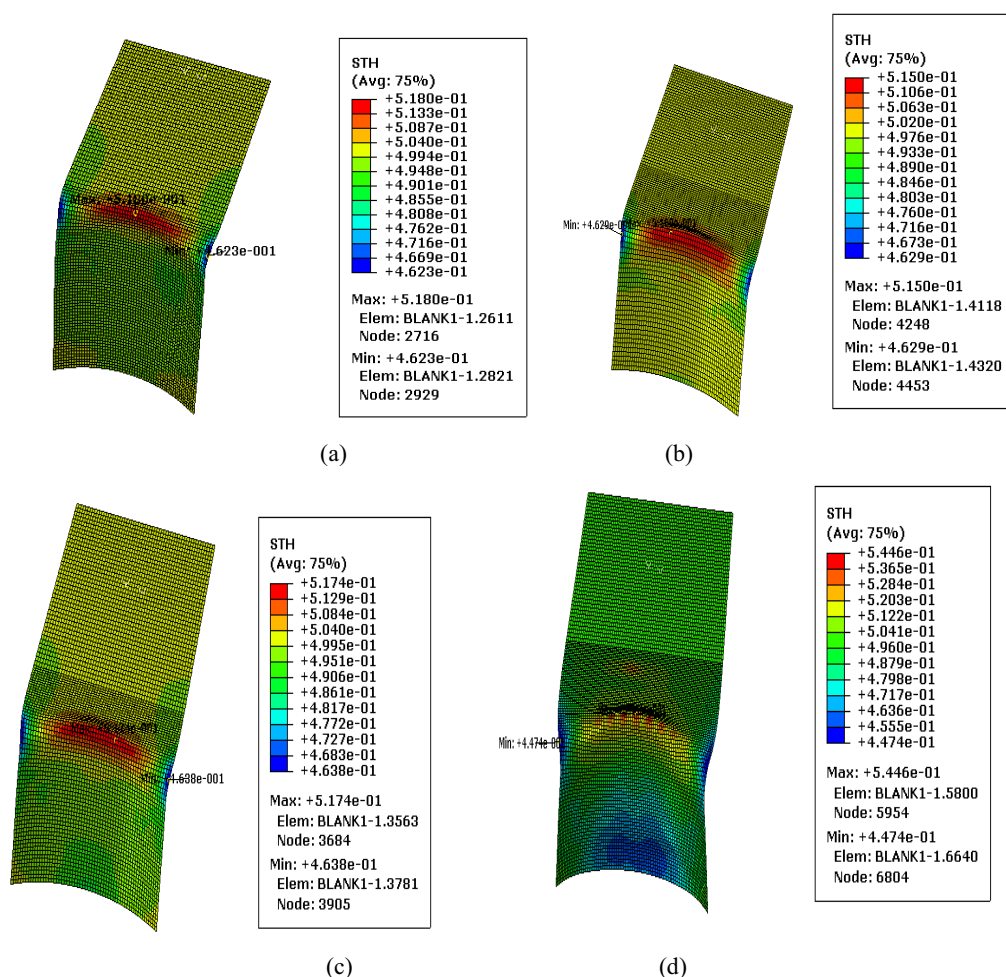
Fig. 21. Effect of width of blank on percentage of thinning(maximum)

Table 3. Effect of different process parameters on percentage of thinning

S.No.	Name of parameter	Value of parameter	Calculation	Maximum Percentage of thinning
1	Initial flange length (mm)	20	$(0.5-0.4630) / 0.5 * 100$	7.40
2		30	$(0.5-0.4623) / 0.5 * 100$	7.52
3		40	$(0.5-0.4623) / 0.5 * 100$	7.54
4		50	$(0.5-0.4623) / 0.5 * 100$	7.54
5	Punch-die clearance (mm)	0.50	$(0.5-0.4620) / 0.5 * 100$	7.60
6		0.75	$(0.5-0.4625) / 0.5 * 100$	7.50
7		1.0	$(0.5-0.4625) / 0.5 * 100$	7.50
8	Blank -holding force (N)	400	$(0.5-0.4653) / 0.5 * 100$	6.94
9		500	$(0.5-0.4641) / 0.5 * 100$	7.18
10		600	$(0.5-0.4638) / 0.5 * 100$	7.24
11	Width of blank (mm)	40	$(0.5-0.4620) / 0.5 * 100$	7.60
12		50	$(0.5-0.4523) / 0.5 * 100$	9.54
13		60	$(0.5-0.4474) / 0.5 * 100$	10.52

length, blank-holding force and width of blank whereas it decreases with increase in punch-die clearance. Out of these four process parameters, width of blank is the most dominating parameter which significantly influence the percentage of thinning (maximum). The higher is the width of blank, initial flange length and blank holding force, greater will be the percentage thinning (maximum) in stretch flange. The increment in percentage of thinning with increment in the width of blank, initial flange length and blank holding force and decrement in punch-die

clearance is basically occurring due to the combined effect of coefficient of friction in conjunction with these process parameters such as width of blank, initial flange length and blank holding force. The percentage of thinning decreases with increase in punch-die clearance as in this the effect of coefficient of friction diminishes. Therefore, coefficient of friction plays an important role again here in increment as well as decrement in percentage thinning in stretch flange. Fig. 22 shows the typical contour plots of percentage of thinning for initial flange



**Fig. 22.** Effect of process parameters on percentage of thinning (maximum) (a) initial flange length (L= 50 mm) (b) punch-die clearance (c = 0.75 mm) (c) blank-holding force (BHF = 600N) (d) width of blank (w = 60 mm)

length (L=50 mm), punch-die clearance (c=1 mm), blank-holding force (BHF = 600 N) and width of blank (w=60 mm) respectively. It is clear from the contour plots that maximum thinning occurs when the blank is bending into die because as the blank is bending into die, circumferential tensile stresses are generated along die profile radius, which are greatest at the edge of sheet. Therefore maximum thinning is reported at edge of sheet due to bending of blank into die.

#### 4. CONCLUSIONS

This paper presents the effect of process parameters such as initial flange length, punch-die clearance, blank holding force and width of

sheet using finite element analysis. Mesh convergence study has been carried out to ascertain the accuracy of present FEM results. Width of sheet is found to be major parameter which significantly affects the formability of stretch flanging process. It is found that maximum thinning (%) increases approximately by 38 % with increase in width of sheet. The greater the width of sheet, higher will be the change in thickness at the end of flange. Initial flange length has a negligible effect on maximum thinning (%) as it increases only by 2% with increase in initial flange length. Punch-die clearance also has a negligible effect on maximum thinning (%) as it decreases by 3 %. Blank holding force has a reasonable effect on maximum thinning (%), as it increases by 5%

with increase in blank holding force. There are number of parameters in stretch flanging process which still need to be studied. In the present analysis, constant blank holding forces are utilized. The following are the major outcomes of research work:

- The circumferential strain and shell thickness decreases with decrease in initial flange length while radial strain increases with decrease in initial flange length.
- The circumferential strain and shell thickness decreases, with decrease in punch-die clearance whereas radial strain increases with decrease in punch-die clearance.
- The circumferential strain and shell thickness decreases with increase in blank-holding force while radial strain increases with increase in blank-holding force.
- The radial strain increases with increase in width of sheet along free edge up to centre of the sheet while circumferential strain decreases with increase in width of sheet.
- The maximum percentage of thinning increases with increase in initial flange length, blank-holding force, width of sheet while it decreases with increase in punch-die clearance.

## REFERENCES

1. Sajadi, S. A., Ebrahimi, R. and Moshksar, M. M., "An analysis on the forming characteristics of commercial pure aluminum AA 1100 in radial forward extrusion process". *Iran. J. Mater. Sci. Eng.*, 2009, 6(1), 1-6.
2. Taheri, A. K., Kazeminezhad, A. and Tieu, K., "Theoretical and experimental evaluation of dislocation density in a workpiece after forming". *Iran. J. Mater. Sci. Eng.*, 2007, 4(1), 1-8.
3. Eshghi, E. and Kadkhodayan, M., "Sheet electromagnetic forming using convex punch instead of concave die". *Iran. J. Mater. Sci. Eng.*, 2016, 13(2), 1-9.
4. Feng, X., Zhongqin, L., Shuhui, L. and Weili, X., "Study on the influences of geometrical parameters on the formability of stretch curved flanging by numerical simulation". *J. Mater. Process. Technol.*, 2004, 145(1), 93–98.
5. Li, D., Luo, Y., Peng, Y. and Hu, P., "The numerical and analytical study on stretch flanging of v-shaped sheet metal". *J. Mater. Process. Technol.*, 2007, 189(1-3), 262–267.
6. Yeh, F. H., Wu, M. T. and Li, C. L., "Accurate optimization of blank design in stretch flange based on a forward–inverse prediction scheme" *Int. Mach. Tool. Manu.*, 2007, 47(12-13), 1854–1863.
7. Chen, Z., Worswick, M. J., Pilkey, A. K. and Lloyd, D. J., "Damage percolation during stretch flange forming of aluminum alloy sheet". *J. Mech. Phys. Solids.*, 2015, 53(12), 2692-2717.
8. Butcher, C., Chen, Z. and Worswick, M., "A lower bound damage-based finite element simulation of stretch flange forming of Al–Mg alloys". *Int. J. Frac.*, 2006, 142(3-4), 289-298.
9. Simha, C. H. M., Grantab, R. and Worswick, M. J., "Application of an extended stress-based forming limit curve to predict necking in stretch flange forming". *J. Manuf. Sci. E-T ASME*, 2008, doi:051007-1- 051007-11(2008).
10. Dewang, Y., Hora, M. S. and Panthi, S. K., "Finite element analysis of non-axisymmetric stretch flanging process for prediction of location failure", *Procedia Materials Science* 5, 2014, 2054-2062.
11. ASTM E8/E8M-11(2011), "Standard test methods for tension testing of metallic materials", ASTM International, West Conshohocken, PA.